

Lecture 4. Measurements without contact in heat transfer.

Part B: Quantitative Infrared Thermography

H. Pron¹, L. Ibos²

¹ **Université de Reims / ITheMM EA 7548, Reims**

E-mail: herve.pron@univ-reims.fr

² **Université Paris-Est Créteil / CERTES EA 3481, Créteil, France**

E-mail: ibos@u-pec.fr

Abstract. The main objective of this lecture is to make the end users aware of the various physical phenomena and especially of the errors frequently met during temperature and heat flow measurement by infrared thermography. For that purpose, this chapter will present the three aspects of a quantitative infrared measurement that are spatial, temporal and thermal resolution. First, the spatial resolution will be discussed, showing that an increase of the matrix size does not necessarily induce an improvement of the spatial resolution. Then, a paragraph is especially dedicated to the temporal aspects, as far as many applications require at least stable frequency to high speed imaging. Last but not least, the calibration of the systems is discussed, showing that accurate measurements often need a specific home-made thermal calibration.

1. Foreword: why it is important to well know your equipment?

Prior to any quantitative measurement using an infrared device, it is important to be aware of the limitations of the technique, but also of the transfer function of the device. Some work, concerning either the thermography technique [1,2] or the associated metrology [3-6] are available in the literature.

There are three major points of necessary characterization of the devices: inaccuracies of the calibration, spatial non-uniformity, and irregular time sampling can lead to false parameter estimation.

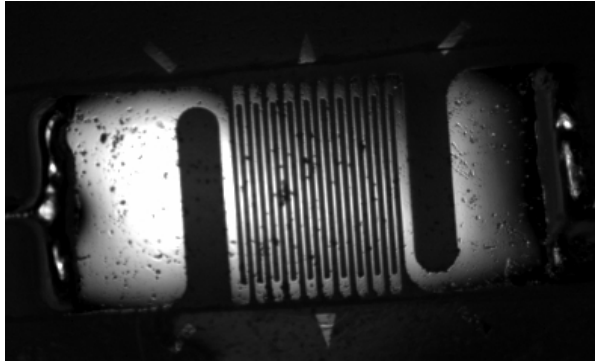


Figure 1. Strain gauge (tracks of approximately 20 μm) observed with a “M1” lens.

2. Spatial resolution

The focal plane array technology has indubitably led to improvements in image quality (Figure 1 hereafter). However, the quality of an image can be considered either from the point of view of the aesthetic, or from the one of the metrology. Unfortunately, these two approaches are rarely compatible...

In order to ensure to obtain reliable measurements, the independence of each sensor relatively to its neighbors must be checked. One of the most current tests for characterizing such equipment is the Slit Response Function (SRF) test: the camera focuses on a thermal side-cooled slit of variable width, placed in front of a hot plate; the following contrast function is then studied:

$$FRF = \frac{V(x) - V_{\min}}{V_{\max} - V_{\min}}, \quad (\text{eq 1})$$

where $V(x)$ is the value recorded for a slit width equal to x , V_{\max} is the value recorded when the slit is wide open ($x \rightarrow \infty$) and V_{\min} is the recorded value on the cooled part (Figure 2a). In general, it is assumed that, for 320 x 240 pixel cameras, to obtain a good measurement the object must be projected on at least two detectors. Thus, with a lens magnification of 1 (“M1”) and a matrix periodicity of 30 μm , one obtains truly independent information only at each step of 60 μm .

A study of this SRF for different positions clearly shows (Figure 2) that the pixels are quite more correlated on the edges of the array than in the center. Note that there is indeed a problem of correlation between close measurement points, i.e. on the one hand, only the contrast (and by no means the average value) is affected and, on the other hand, there is convolution of the thermal scene by this response function. Consequently, a simple geometrical correction (e.g. of repositioning of the points in the image, or amplification and/or offsets applied to each pixel) is necessary to recover the real quantitative image of the scene, in addition to a deconvolution procedure. A possible restoration procedure of thermal images based on the characterization of the Modulation Transfer Function of the camera was proposed in [7].

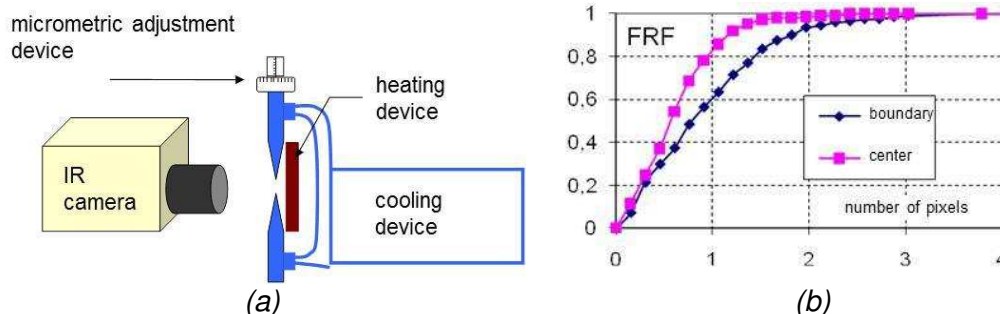


Figure 2. (a) Slit Response Function; (b) SRF near the edge of the array compared to SRF at the centre (CEDIP IRC 320-4 LW camera)

3. Temporal analysis

First, it seems to be necessary to remind, before any characterization, some important definitions concerning this technology.

- Integration time: this duration corresponds to the part of the image period during which the detectors are effectively loading their associated capacitors; so, they measure the external infrared radiation during the integration time only. Any user should be aware that this duration is very short (often about one millisecond), compared to the frame period (typically about 10 or 20 ms for a full window): most of the frame period is dedicated to the reading of the stored electrical signals. In some situations, this is a problem since very quick phenomena can occur during this “blind” phase.

- Multiplexing duration: the reading of the different pixels is not simultaneous; according to the considered device, the pixel signals can be read by up to four channels, at a sampling rate of a few MHz (f_{ADC} hereafter). Then, t_s being the settle time, the maximum frame frequency can be simply obtained by:

$$f = \left(t_i + \frac{n_r \times n_c}{N \times f_{ADC}} + t_s \right)^{-1} \quad (\text{eq 2})$$

where:

n_r is the number of rows,
 n_c the number of columns,
 and N the number of channels.

The integration time t_i is the duration during which the radiation coming from the thermal scene is collected by the detectors of the camera. Consequently, it determines the ultimate temporal resolution of the device. As the image transfer time to the storage memory or to the hard disk is often much higher than the integration time (several milliseconds compared to some tenths or hundreds of microseconds), the detector thus does not see the scene during most of the time, which is particularly penalizing for observing fast phenomena.

Regardless of the problems connected to the integration time, the temporal analysis can be disturbed by the absence of some images in the stored sequence. Depending on the devices,

a temporal shift of one or two images can occur at the beginning of the sequence. This is due to the fact that the first stored image corresponds to the one that was captured when the starting order occurred, not the actual image at the beginning of the sequence; sometimes, due to pre-processing, the temporal shift can be of two images. Then, on condition that the user is aware of this fact, a simple sequence shift is enough to correct this edge effect.

The second, more penalizing, problem is the absence of some images within a sequence. This problem is relatively unimportant in terms of visualization, but can become critical in the data processing when time is highly involved. Algorithms that are compatible with variable acquisition frequencies are then required. To count and isolate times from the missing images, it is possible to directly read time information in the files from the camera, provided that they have been accurately stored, *i.e.* sufficient with respect to the acquisition frequencies used. Depending on the camera model, the number of images missing can thus range from one to several dozens.

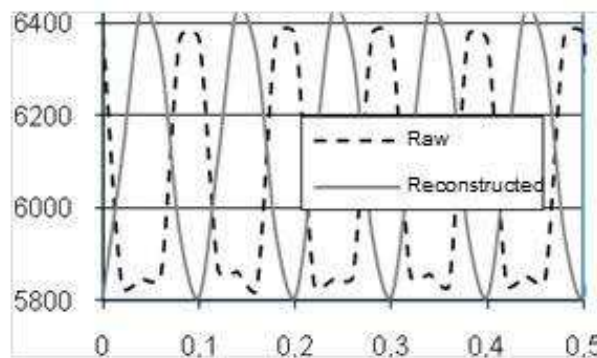


Figure 3. Errors induced by the missing images in lock-in thermography: amplitude is not really affected but phase is strongly distorted

Figure 3 presents the artefacts observed in the case of a numerical lock-in procedure applied to a series of 30 images in which only two images are missing. If the amplitude is not very affected, the phase has a completely erratic behaviour, and takes a value that depends directly on the number and the phase of the missing images.

4. Thermal aspects

4.1. Thermal noise and thermal drift

The infrared devices usually used in R&D are cooled at approximately 80 K in order to reduce radiation in the vicinity of the infrared sensors. In new-generation IR cameras, a Stirling cycle engine has replaced liquid nitrogen cooling systems of older cameras. Though the cameras have thus gained in portability, this new system has a non-negligible drawback: the cooling, which was quasi-instantaneous with nitrogen, now requires at least 10 min before any measurement is possible (figure 4a).

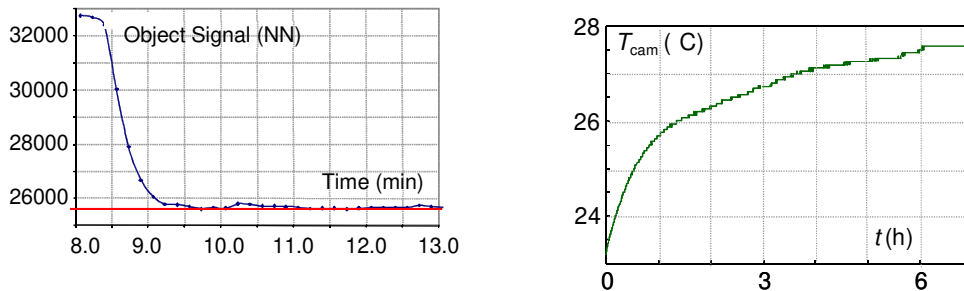


Figure 4. (a) Cooling CEDIP IRC320-4LW, (b) thermal drift CEDIP JADE III

In addition, once the cooling is achieved, a slow drift of about 1 to 5 mK per second can occur with certain materials, sometimes over durations reaching a few hours (figure 4b). This temperature drift is mainly due to the evolution of the internal temperature of the camera, and modify the sensor responses, so it is appropriate in several situations to wait until the camera temperature is stabilized, or to take this internal drift into account in the conversion of the digitized signal into temperature (Compensated NUC). In addition, certain lower quality materials have instabilities of 0.5 or even 1 K, which that is incompatible with quantitative measurements.

4.2. Environment thermal stability

The signal measured by a camera comes primarily from the object (assumed to be gray and opaque in the camera's spectral range), but also, to a lesser extent (in the most favorable conditions), from the environment and atmosphere (figure 5). If the environment can be considered as an integral radiator of temperature T_{env} and if the atmosphere between the target and the camera is isothermal at the temperature T_{atm} , considering a coefficient of transmission τ_{atm} , the measured intensity L_{mes} can be formulated as a function of the intensity L^0 of a blackbody at the object temperature:

$$L_{mes} = \tau_a \cdot \epsilon \cdot L^0(T_{obj}) + \tau_a (1 - \epsilon) L^0(T_{env}) + (1 - \tau_a) L^0(T_{atm}) \quad (\text{eq 3})$$

For short distance measurements (about a few tenths of cm), the atmosphere can reasonably be considered as being transparent, and thus:

$$L_{mes} = \epsilon L^0(T_{obj}) + (1 - \epsilon) L^0(T_{env}) \quad (\text{eq 4})$$

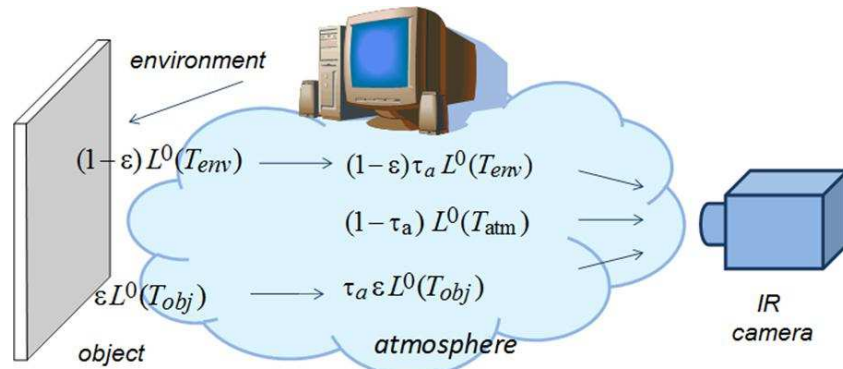


Figure 5. Simplified radiometric balance

This equation shows that the environment must be reasonably well controlled in order to limit the influence of parasitic radiation (reflection from a radiator or any other radiative IR source, or even from the operator!). This precaution is all the more important when the measured temperature increases are minor. In addition, using a high emissivity coating (thus of low reflectivity) is obviously advantageous to minimize the parasitic flow/object flow ratio.

Along the same lines, note also the presence of the Narcissus effect (reflection of the cold detector on the scene), which is often observed when using a macro lens (e.g. lens magnification of 1, [8]). Usually, this is only an offset map which is superimposed on the scene, and which can thus be offset by subtraction of a reference image. Last but not least, possible environmental instabilities could modify the exchange conditions between the sample and its environment and thus must be taken into account, especially when there are strong temperature variations over time.

4.3. Thermal calibration

In order to obtain reliable results, the user must, first of all, be confident in the apparatus calibration. Most of the time, infrared devices have their own setting and acquisition applications, including data-processing applications for digitizing, non-uniformity corrections, display, basic operations...

Generally, the calibration laws used by manufacturers suppose the sensor's response is linear, and consider the differences between the pixels' responses only as distributions of gains and offsets. The calibration of the device consists then in two distinct operations: the calibration of the average of a central area, and the application of maps of gains and offsets to link the response of each pixel to the one of the average of the sensor matrix. This second operation is called "Non-Uniformity Correction" (NUC).

The calibration law is generally taken in the form of a 2 or 3-degree polynomial, or a Planck-type law.

$$L_m(T) = aT^2 + bT + c \quad (\text{eq 5})$$

$$L_m(T) = \frac{R}{\left[\exp\left(\frac{B}{T}\right) - F \right]} + \text{Offset} \quad (\text{eq 6})$$

Where (a, b, c) or $(R, B, F$ and $Offset)$ are parameters identified during the calibration, and L_m the intensity measured by the camera, expressed in arbitrary units.

The gains and offsets maps are computed so as to obtain uniform distributions of digitized fluxes for two specific images of uniform thermal scenes taken at two different temperatures; these two scenes are generally obtained by means of an extended blackbody. Recently, some manufacturers proposed to go further, by linking the values of the gain and offset maps to an “internal temperature” of the camera, in order to compensate the thermal drifts associated with the heat produced by the internal electronics and the heat exchanges between the camera and its environment. This “advanced” non-uniformity correction is often called “Compensated Non-Uniformity Correction”: CNUC.

Moreover, sensor matrices always include some defective pixels (generally less than 0.5%), that can be saturated pixels, noisy pixels, or even “dead” pixels. They are localized using criteria dealing mainly with the discrepancy with respect to the mean response (in terms of digitized flux, gain, offset, etc.). Manufacturers propose to replace the value of these pixels by the one of their nearest non-defective neighbour (Bad Pixel Replacement, or BPR procedure), that induces a complete local correlation.

The validity of the standard calibrations can be easily checked out by observing a given thermal scene with a unique camera, but using different calibrations, associated with different acquisition settings (integration time / measurement range). As an illustration, figure 6 illustrates different observations on a blackbody using different infrared cameras. These two illustrations show that it is appropriate, if possible, to use the centre of the matrix and the middle of the calibration range when using the manufacturer’s calibration laws. If the application needs a wider measurement area, it could be convenient to take into account the dispersion of the measured values in the data treatment procedure.

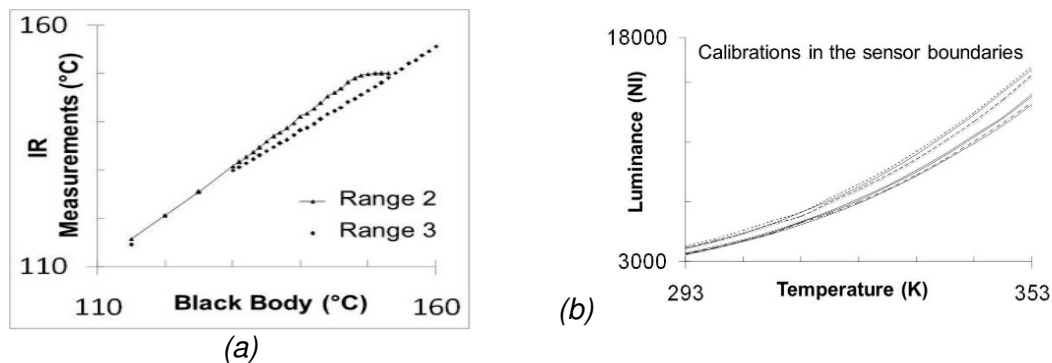


Figure 6. Check of the calibration using an extended black body: (a) Comparison between two ranges of a single camera (FLIR SC1000), (b) Comparison between several pixel responses (CEDIP IRC 320-4LW) of the array.

If the specifications on the measurement accuracy are more stringent than one Kelvin, or if the independence of the measurement is a critical parameter for the later data processing, another solution is to be found. The most logical one consists in performing a customized calibration of the whole sensor matrix with testing conditions and camera configuration (integration time, windowing, etc.) similar to those used for the application, fitting the behaviour of each detector independently.

This calibration overcomes the limitations inherent to the NUC (or CNUC) and BPR procedures (linearity assumption valid further enough from saturation for the NUC, introduction of a strong spatial correlation between neighbouring pixels for the BPR operation...). However, it requires a high-uniformity extended blackbody so as to have a uniform radiation source at different temperature levels covering the whole range of the future application.

Once more, as in the standard global calibration procedure, the calibration law of each pixel can be chosen as a polynomial or as a Planck-like function, but the constant will be arrays of coefficients, the size of which being the one of the infrared matrix itself. These calibration coefficients are obtained by approximating, generally in the least squares sense, the couples (digitized radiation–temperature) by the chosen calibration function.

Defective pixels are then localized using a criterion for measuring the mismatch between the calibrated and specified temperature. The BPR operation is not performed: temperatures of the defective pixels are not taken into account in the subsequent data-processing. A specific pixel-to-pixel calibration is detailed in [9,10].

5. Conclusion

Accurate temperature measurement by radiative means is not an easy task. Many parameters have to be evaluated beforehand for extracting the surface emitted radiance from the measured radiance (atmospheric contributions: self-emission and attenuation, environments radiance reflections). One then faces the problem of temperature-emissivity separation. This underdetermined problem requires that some knowledge about the emissivity of the tested

material is introduced. A general thought is that by adding spectral measurements at one or several other wavelengths would help identifying the temperature. The underdetermined nature of the problem is however maintained. Introducing a model for the emissivity spectral profile is often a misleading idea: high systematic errors unavoidably emerge when the model doesn't perfectly match to the real emissivity profile. Having some knowledge on emissivity *magnitude* helps much than imposing an arbitrary *shape* model.

6. References

- [1] Gaussorgues G, "La Thermographie Infrarouge - Principes, Technologie, Applications", 4^{ème} Édition, Tec & Doc Lavoisier, 1999 (in french)
- [2] Pajani D, "Mesure Par Thermographie Infrarouge", Editeur ADD, EAN13 978293417107, 1989 (in french)
- [3] Pron H, Menanteau W, Bissieux C, Beaudoin J-L, "Characterization of a focal plane array (FPA) infrared camera", QIRT 2000 (Eurotherm No. 64), Reims, 18-21 juillet 2000, pp 112-117
- [4] Bissieux C, Pron H et Henry J-F "Pour de véritables caméras matricielles de recherche", revue Contrôles Essais Mesures, janvier 2003, vol n°2, pp. 39-41 (in french)
- [5] Pron H, Laloue P, Henry J-F, L'ecolier J, Bissieux C et Nigon F, "Caractérisation de caméras infrarouges à matrice de détecteurs", 3^{ème} Colloque Interdisciplinaire en Instrumentation, ENS Cachan, 29-30 janvier 2004, vol. 2, pp. 215-222 (in french)
- [6] Pron H and Bissieux C, "Focal Plane Array infrared cameras as research tools", QIRT Journal, Vol. 1(2), 2004, pp. 229-240
- [7] Datcu S, Ibos L, Candau Y, Mattéi S, Frichet J-C, "Focal plane array infrared camera transfer function calculation and image restoration", Optical Engineering, Vo. 43(3), 2004, pp. 648-657
- [8] Poncelet M, Witz J-F, Pron H, Watrisse B, "A study of IRFPA camera measurement errors: radiometric artefacts", QIRT Journal. Vol. 8(1), 2011, pp. 3-20
- [9] Honorat V, Moreau S, Muracciole J-M, B. Watrisse B, Chrysochoos A, "Calorimetric analysis of polymer behaviour using a pixel calibration of an IRFPA camera", QIRT Journal, Vol. 2(2), 2005, pp.153-172
- [10] Pron H, Bouache T, "Alternative thermal calibrations of Focal Plane Array infrared cameras", QIRT Journal, Vol. 13(1), 2016, pp 94-108